Published in IET Microwaves, Antennas & Propagation
Received on 27th April 2009
Revised on 6th July 2009
doi: 10.1049/iet-map.2009.0198

ISSN 1751-8725

Coarse models for efficient space mapping optimisation of microwave structures

S. Koziel[1] *J.W. Bandler*[2,*]

[1]*Engineering Optimization & Modeling Center, School of Science and Engineering, Reykjavik University, Kringlunni 1, IS-103 Reykjavik, Iceland*
[2]*Simulation Optimization Systems Research Laboratory, Department of Electrical and Computer Engineering, McMaster University, Hamilton, ON, Canada L8S 4K1*
[*]*Bandler Corporation, Dundas, ON, Canada L9H 5E7*
E-mail: koziel@ru.is

Abstract: It follows from both theoretical results and practical observations that the coarse model is one of the most critical components of the space mapping optimisation process, affecting both the algorithm's ability of finding a high-quality design, and its computational complexity. A good coarse model should be a good representation of the fine model and, at the same time, it should be computationally cheap. The first property not only ensures the quality of the final design but also good convergence properties of the algorithm, so it also affects the computational complexity of the optimisation process through reducing the number of fine model evaluations required to find the solution. The second property ensures that the overhead related to parameter extraction and surrogate optimisation is small or even negligible. This study discusses techniques for creating computationally cheap and reliable coarse models. The approaches the authors present include interpolated models, multi-coarse-model techniques and the use of built-in capabilities of the coarse model simulator. The authors provide examples involving microwave design optimisation problems.

1 Introduction

Automated design optimisation of radio frequency and microwave structures faces the substantial obstacle of the high computational cost of the objective function, typically evaluated using full-wave electromagnetic simulators. Cheap sensitivity data are normally unavailable; consequently, direct optimisation is usually computationally prohibitive. So-called surrogate-based optimisation methods [1–4] may alleviate these problems. Here, the direct optimisation of the original, computationally expensive structures ('fine' models) is replaced by the iterative optimisation and updating of significantly cheaper surrogate models.

A notable example of surrogate-based optimisation is space mapping (SM) [5–10], a technique originally developed to deal with time-intensive design problems in microwave engineering, now increasingly popular in other arenas [11–14]. Here, the surrogate is built on an underlying physically based 'coarse' model of the respective structure. The coarse model addresses the same physical phenomena as the fine model but in a simplified way (for example, lumped element circuit equivalent against full-wave electromagnetic model). This facilitates good alignment between the fine model and the space mapping surrogate using a modest amount of fine model data, as well as exploiting the excellent prediction capability of the surrogate. These advantages are not enjoyed by functional surrogate modelling techniques such as polynomial approximation, radial basis functions or kriging [15–17], which is probably why surrogate-based optimisation methods exploiting functional surrogates, for example, [1, 4, 18] have not been widely adopted in microwave engineering so far.

Substantial effort has been devoted to improving the efficiency of space mapping optimisation through new algorithms and new space mapping surrogate model types [6–8, 19, 20], improving the convergence properties of the

space mapping algorithms [21, 22], as well as designing assessment methods allowing automatic or semi-automatic selection of the surrogate model type for a given design problem [23–25]. Still, the quality of the underlying coarse model is probably the most important factor determining the performance of a space mapping algorithm. The coarse model should be as good a representation of the fine model as possible but also significantly less expensive than the fine model [6, 7, 23]. Under such conditions, the space mapping algorithm can reach a satisfactory solution after a few fine model evaluations without significant overhead related to operations on the coarse/surrogate model.

Available coarse models are often cheap but inaccurate, for example, a circuit equivalent of the microwave structure, or accurate but expensive, for example, a structure evaluated using the same simulator as the fine model but with a coarser mesh. In the first case, the space mapping optimisation process suffers from the overhead of excessive fine model evaluations needed to find a good solution, or the process may even fail to find a satisfactory solution. In the latter case, the cost of solving the parameter extraction and surrogate optimisation sub-problems may be comparable with the cost of fine model evaluation, or may even determine the total cost of the space mapping optimisation.

In this paper, we review and contrast recently published methods of creating computationally cheap and reliable coarse models that allow us to take full advantage of the space mapping concept. The paper is organised as follows. In Section 2 we recall the concept of space mapping and discuss the role of coarse model in the optimisation process. In Section 3 we discuss the interpolated coarse models technique [26], multi-coarse-model space mapping [27] and some software techniques based on built-in optimisation capabilities of the coarse model simulator [28]. All of these approaches have been incorporated in our Space Mapping Framework (SMF) system [29]. Their performance is illustrated using microwave design optimisation problems. Section 4 concludes the paper.

2 Space mapping optimisation: formulation and practical issues

In this section we formulate the space mapping optimisation algorithm and examine factors determining its performance. We also discuss the importance of the computational complexity and accuracy of the underlying coarse model.

2.1 Formulation of space mapping

Let $\boldsymbol{R}_{\mathrm{f}}(\boldsymbol{x})$ denote the response vector of a fine model corresponding to a design variable vector $\boldsymbol{x}$. In the microwave arena, $\boldsymbol{R}_{\mathrm{f}}(\boldsymbol{x})$ may represent the magnitude of a transfer function of a filter at a given set of frequencies. The optimisation problem is formulated as follows

$$\boldsymbol{x}_{\mathrm{f}}^{*} = \arg\min_{x} U(\boldsymbol{R}_{\mathrm{f}}(\boldsymbol{x})) \tag{1}$$

where U is a given merit function, for example, a norm or a minimax function [6]; $\boldsymbol{x}_{\mathrm{f}}^{*}$ is an optimal fine model design to be found.

A space mapping optimisation algorithm generates a sequence of approximate solutions to problem (1), denoted as $\boldsymbol{x}^{(i)}$, $i = 0, 1, 2, \ldots$, and a family of surrogate models $\boldsymbol{R}_{\mathrm{s}}^{(i)}$, so that we have

$$\boldsymbol{x}^{(i+1)} = \arg\min_{x} U(\boldsymbol{R}_{\mathrm{s}}^{(i)}(\boldsymbol{x})) \tag{2}$$

Let $\boldsymbol{R}_{\mathrm{c}}$ denote the response vector of the coarse model that represents the same object as the fine model: less accurate but much faster to evaluate. Surrogate models are constructed from the coarse model so that the misalignment between $\boldsymbol{R}_{\mathrm{s}}^{(i)}$ and the fine model is minimised. $\boldsymbol{R}_{\mathrm{s}}^{(i)}$ is defined as [25]

$$\boldsymbol{R}_{\mathrm{s}}^{(i)}(\boldsymbol{x}) = \bar{\boldsymbol{R}}_{\mathrm{s}}(\boldsymbol{x}, \boldsymbol{p}^{(i)}) \tag{3}$$

where $\bar{\boldsymbol{R}}_{\mathrm{s}}$ is a generic space mapping surrogate model, that is, the coarse model composed with suitable transformations, whereas

$$\boldsymbol{p}^{(i)} = \arg\min_{p} \sum_{k=0}^{i} w_{i.k} \| \boldsymbol{R}_{\mathrm{f}}(\boldsymbol{x}^{(k)}) - \bar{\boldsymbol{R}}_{\mathrm{s}}(\boldsymbol{x}^{(k)}, \boldsymbol{p}) \| \tag{4}$$

is a vector of model parameters and $w_{i.k}$ are weighting factors; a common choice of $w_{i.k}$ is $w_{i.k} = 1$ for all i and all k.

Various space mapping surrogate models are available [6–8]. They can be roughly categorised into four groups: (i) models based on a (usually linear) distortion of coarse model parameter space, for example, input space mapping of the form $\bar{\boldsymbol{R}}_{\mathrm{s}}(\boldsymbol{x}, \boldsymbol{p}) = \bar{\boldsymbol{R}}_{\mathrm{s}}(\boldsymbol{x}, \boldsymbol{B}, \boldsymbol{c}) = \boldsymbol{R}_{\mathrm{c}}(\boldsymbol{B} \cdot \boldsymbol{x} + \boldsymbol{c})$ [6]; (ii) models based on a distortion of the coarse model response, for example, output space mapping of the form $\bar{\boldsymbol{R}}_{\mathrm{s}}(\boldsymbol{x}, \boldsymbol{p}) = \bar{\boldsymbol{R}}_{\mathrm{s}}(\boldsymbol{x}, \boldsymbol{d}) = \boldsymbol{R}_{\mathrm{c}}(\boldsymbol{x}) + \boldsymbol{d}$ [7]; (iii) implicit space mapping, where the parameters used to align the surrogate with the fine model are separate from the design variables, that is, $\bar{\boldsymbol{R}}_{\mathrm{s}}(\boldsymbol{x}, \boldsymbol{p}) = \bar{\boldsymbol{R}}_{\mathrm{s}}(\boldsymbol{x}, \boldsymbol{x}_{\mathrm{p}}) = \boldsymbol{R}_{\mathrm{c}.i}(\boldsymbol{x}, \boldsymbol{x}_{\mathrm{p}})$, with $\boldsymbol{R}_{\mathrm{c}.i}$ being the coarse model dependent on both the design variables $\boldsymbol{x}$ and so-called preassigned parameters $\boldsymbol{x}_{\mathrm{p}}$ (for example, dielectric constant, substrate height) that are normally fixed in the fine model but can be freely altered in the coarse model [30]; (iv) custom models exploiting parameters characteristic to a given design problem; the most characteristic example is the so-called frequency space mapping $\bar{\boldsymbol{R}}_{\mathrm{s}}(\boldsymbol{x}, \boldsymbol{p}) = \bar{\boldsymbol{R}}_{\mathrm{s}}(\boldsymbol{x}, \boldsymbol{F}) = \boldsymbol{R}_{\mathrm{c.f}}(\boldsymbol{x}, \boldsymbol{F})$ [6], where $\boldsymbol{R}_{\mathrm{c.f}}$ is a frequency-mapped coarse model, that is, the coarse model evaluated at frequencies different from the original frequency sweep for the fine model, according to the mapping $\omega \rightarrow f_1 + f_2\omega$, with $\boldsymbol{F} = [f_1\ f_2]^{\mathrm{T}}$.

The basic space mapping types are usually combined, for example, the surrogate model employing both input, output and frequency space mapping types would be as follows: $\bar{\boldsymbol{R}}_{\mathrm{s}}(\boldsymbol{x}, \boldsymbol{p}) = \bar{\boldsymbol{R}}_{\mathrm{s}}(\boldsymbol{x}, \boldsymbol{c}, \boldsymbol{d}, \boldsymbol{F}) = \boldsymbol{R}_{\mathrm{c.f}}(\boldsymbol{x} + \boldsymbol{c}, \boldsymbol{F}) + \boldsymbol{d}$. The rationale

doi: 10.1049/iet-map.2009.0198

for this is that a properly chosen mapping may significantly improve the performance of the space mapping algorithm; however, the optimal selection of the mapping type for a given design problem is not trivial [23–25].

The space mapping optimisation algorithm flow can be described as follows:

Step 1: Set $i = 0$; choose the initial design solution $\boldsymbol{x}^{(0)}$;

Step 2: Evaluate the fine model to find $\boldsymbol{R}_f(\boldsymbol{x}^{(i)})$;

Step 3: Obtain the surrogate model $\boldsymbol{R}_s^{(i)}$ using (3) and (4);

Step 4: Given $\boldsymbol{x}^{(i)}$ and $\boldsymbol{R}_s^{(i)}$, obtain $\boldsymbol{x}^{(i+1)}$ using (2);

Step 5:. If the termination condition is not satisfied go to Step 2; else terminate the algorithm;

Typically, $\boldsymbol{x}^{(0)} = \arg\min\{\boldsymbol{x}: U(\boldsymbol{R}_c(\boldsymbol{x}))\}$, that is, it is the optimal solution of the coarse model: the best initial design normally available. We usually terminate the algorithm when it converges (that is, $\|\boldsymbol{x}^{(i)} - \boldsymbol{x}^{(i-1)}\|$ is smaller than some user-defined value) or when the maximum number of iterations (or, more often, the number of fine model evaluations) is exceeded.

2.2 Coarse model and performance of the space mapping optimisation algorithm

If the surrogate model is a sufficiently good representation of the fine model [23], the space mapping algorithm typically requires a few fine model evaluation to yield a satisfactory solution, substantially less than the number of fine model evaluations reported for any other method. Direct optimisation typically requires dozens or even hundreds of model evaluations for typical microwave engineering design problems. However, we should not expect the final solution found by space mapping to be a local optimum of the fine model unless, for example, first-order consistency conditions between the surrogate and fine models are ensured and convergence safeguards such as trust region methods are used [7].

As mentioned in Section 2.1, the surrogate model is normally a composition of the coarse model and certain (usually linear) mappings selected from a large number of available setups. Work has been done to ease the selection process for a given design problem [23–25]. However, regardless of the mapping choice, coarse model accuracy is what principally affects the performance of the space mapping design process.

We can quantify the quality of the surrogate model through rigorous convergence conditions [7, 23]. These conditions, although useful for developing more efficient space mapping algorithms and automatic surrogate model selection techniques, cannot usually be verified because of the limited amount of data available from the fine model. In practice, the most important criterion for assessing the quality or accuracy of the coarse model is still visual inspection of the fine and coarse model responses at certain points and/or examining absolute error measures such as $\|\boldsymbol{R}_f(\boldsymbol{x}) - \boldsymbol{R}_c(\boldsymbol{x})\|$.

The coarse model affects the performance of the space mapping algorithm in two ways. The first stems from accuracy. Coarse model accuracy (more generally, the accuracy of the space mapping surrogate [23]) is the main factor that determines the efficiency of the algorithm in terms of finding a satisfactory design. The more accurate the coarse model, the smaller the number of fine model evaluations necessary to complete the optimisation process. If the coarse model is insufficiently accurate, the space mapping algorithm may need more fine model evaluations or may even fail to find a good quality design.

The second important characteristic is evaluation cost. It is essential that the coarse model be significantly computationally cheaper than the fine model because both parameter extraction (4) and surrogate optimisation (2) require large numbers of coarse model evaluations. Ideally, the evaluation cost of the coarse model should be negligible when compared to the evaluation cost of the fine model, in which case the total computational cost of the space mapping optimisation process is merely determined by the necessary number of fine model evaluations. If the evaluation time of the coarse model is too high, say, larger than 0.1%–1% of the fine model evaluation time, the computational cost of surrogate model optimisation and, especially, parameter extraction, start playing important roles in the total cost of space mapping optimisation and may even determine it.

We summarise this discussion as follows. To ensure efficiency of the space mapping optimisation process, the underlying coarse model should be accurate and computationally cheap. These requirements are usually complementary. Coarse models based on analytical formulas are the fastest but also inaccurate whereas coarse models based on circuit equivalents are more accurate yet computationally more expensive. Accurate coarse models can be obtained when the same simulator is used to evaluate both the fine and coarse models, with the coarse model simulated using a coarse mesh. In such cases, however, the evaluation cost of the coarse model is usually rather high necessitating special measures to reduce the relative computational overhead of the parameter extraction and surrogate optimisation (see, for example, [31]).

3 Improved coarse models for efficient space mapping optimisation

In this section we discuss methods of creating fast, accurate coarse models that can be successfully applied in the microwave arena. We aim at decreasing the cost of the original coarse models with no or minor degradation of their accuracy through certain interpolation techniques

(Section 3.1) or employing the optimisation capabilities of the coarse model simulator (Section 3.3) or at improving the accuracy of the existing models without increasing the computational cost (Section 3.2).

3.1 Interpolated coarse models

We assume here that the original coarse model, which is accurate but too expensive to be efficiently used in a space mapping algorithm directly, is evaluated on a relatively coarse simulation grid and then interpolated to obtain a response for off-grid values. The resulting interpolated coarse model is fast, requires a small number of evaluations of the original coarse model to be established and retains, to some extent, the accuracy of the original model [26].

We let $\boldsymbol{R}_c: X \rightarrow R^m$, $X \subseteq R^n$, be an original coarse model typically evaluated by the same simulator as the fine model, but using a coarse mesh. Let G be a grid $G(\boldsymbol{\lambda}) = \{[z_1\lambda_1\ z_2\lambda_2\ \ldots\ z_n\lambda_n]^T: z_i \in Z,\ i = 1, \ldots, n\}$, where $\boldsymbol{\lambda} = [\lambda_1\ \lambda_2 \ldots\ \lambda_n]^T$ is an user-defined grid size and Z denotes the set of integers; n is the number of design variables. Grid G divides R^n into hypercubes with points $\boldsymbol{y} \in G(\boldsymbol{\lambda})$ being corners of these hypercubes. For each $\boldsymbol{y} \in G(\boldsymbol{\lambda})$ we define $c(\boldsymbol{y}) = [y_1 + \lambda_1/2\ y_2 + \lambda_2/2 \ldots y_n + \lambda_n/2]^T$ as the centre of the corresponding hypercube, and denote by $H(\boldsymbol{y})$ the hypercube itself. Fig. 1 shows an example of the grid and hypercubes for $n = 2$.

With each $\boldsymbol{y} \in G(\boldsymbol{\lambda})$ we associate a base set $X_B(\boldsymbol{y})$, which is a set of points located in the hypercube with centre $c(\boldsymbol{y})$. We will denote by $R_B(\boldsymbol{y})$ a set of responses of the original coarse model $\boldsymbol{R}_c$ evaluated at points from $X_B(\boldsymbol{y})$.

Let $F(\cdot, X_B, R_B)$ be the function interpolating the data pairs (X_B, R_B). $F(\boldsymbol{x}) = F(\boldsymbol{x}, X_B, R_B)$ denotes the value of the function F at point $\boldsymbol{x}$.

For each $\boldsymbol{x} \in R^n$ we define $s(\boldsymbol{x}) \in G(\boldsymbol{\lambda})$ as $s(\boldsymbol{x}) = [\lambda_1 \cdot \lfloor x_1/\lambda_1 \rfloor \ldots \lambda_n \cdot \lfloor x_n/\lambda_n \rfloor]^T$, which 'rounds' $\boldsymbol{x}$ to one of the grid points.

We define an interpolated coarse model $\bar{\boldsymbol{R}}_c$ as follows

$$\bar{\boldsymbol{R}}_c(\boldsymbol{x}) = F(\boldsymbol{x}, X_B(s(\boldsymbol{x})),\ R_B(s(\boldsymbol{x}))) \tag{5}$$

The interpolation function F can be realised in various ways.

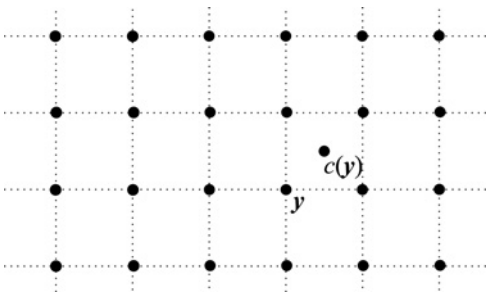

Figure 1 *Grid example for the two-dimensional case [26]*

Here, we employ fuzzy systems, a technique successfully used in the computer-aided design of microwave structures by other authors (for example, [32–34]). In order to ensure continuity of the model $\bar{\boldsymbol{R}}_c$ our fuzzy-system interpolation is based on points located at the corners of the hypercubes defined by the grid G. In particular, we have $X_B(\boldsymbol{y}) = \{\boldsymbol{x}: \boldsymbol{x} = [y_1 + e_1\lambda_1 \quad y_2 + e_2\lambda_2 \quad y_n + e_n\lambda_n]^T,\ e_i \in \{0, 1\},\ I = 1, 2, \ldots, n\}$. An example of the base set for $n = 2$ is shown in Fig. 2. Note that the number of base points is $N = 2^n$.

We use a fuzzy system with triangle membership functions and centroid defuzzification [35]. The fuzzy system uses data pairs $(\boldsymbol{x}^k, \boldsymbol{R}^k)$, where $\boldsymbol{x}^k \in X_B(\boldsymbol{y})$ and $\boldsymbol{R}^k = \boldsymbol{R}_c(\boldsymbol{x}^k)$, $k = 1, 2, \ldots, N$. In our realisation, each interval $[y_i,\ y_i + \lambda_i]$, $I = 1, 2, \ldots, n$, contains only one fuzzy region (that is, the whole interval). Membership functions for ith variable are defined as shown in Fig. 3.

Having defined membership functions we need to generate fuzzy rules from the given data pairs. We use if–then rules of the form IF $\boldsymbol{x}^k$ is in $H(\boldsymbol{y})$ THEN $\boldsymbol{z} = \boldsymbol{R}^k$, where $\boldsymbol{z}$ is the output of the rule. At the level of vector components this means

$$\text{IF } x_1^k \text{ is in } [y_1, y_1 + \lambda_1] \text{ AND } x_2^k \text{ is in } [y_2, y_2 + \lambda_2] \text{ AND } \ldots$$
$$\ldots \text{AND } x_n^k \text{ is in } [y_n, y_n + \lambda_n] \text{ THEN } \boldsymbol{z} = \boldsymbol{R}^k \tag{6}$$

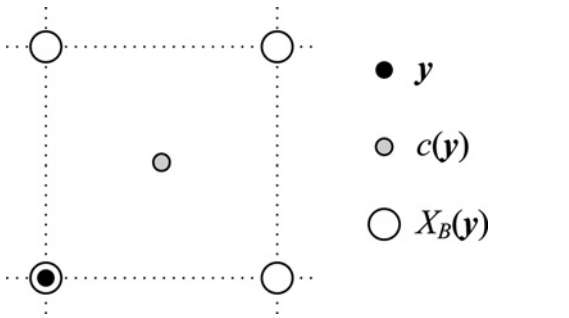

Figure 2 *Example of the base set for fuzzy-system interpolation, n = 2 [26]*

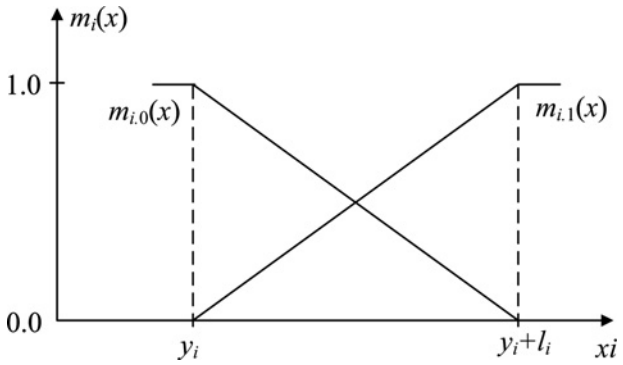

Figure 3 *Input interval $[y_i,\ y_i + \lambda_i]$ and the corresponding membership functions [26]*

doi: 10.1049/iet-map.2009.0198

where x_i^k, $i = 1, \ldots, n$, are components of vector $\boldsymbol{x}^k$. In our case all N rules are conflicting because they have the same IF part but a different THEN part. However, each rule has a different set of associated membership functions. In particular, if $x_j^k = y_j$ then the membership function associated with component j of the kth rule is $m_{j.0}$, otherwise it is $m_{j.1}$.

Each rule has a degree that is assigned in the following way. For the rule 'IF x_1^k is in $[y_1, y_1 + \lambda_1]$ AND x_2^k is in $[y_2, y_2 + \lambda_2]$ AND ... ... AND x_n^k is in $[y_n, y_n + \lambda_n]$ THEN $\boldsymbol{z} = \boldsymbol{R}^k$', the degree of this rule for any $\boldsymbol{x} = [x_1\ x_2 \ldots x_n]^{\mathrm{T}} \in H(\boldsymbol{y})$, denoted by $D_k(\boldsymbol{x})$, is defined as

$$D_k(\boldsymbol{x}) = \prod_{j=1}^{n} m_{j.e_j^k}(x_j) \tag{7}$$

where $e_j^k \in \{0, 1\}$, $j = 1, 2, \ldots, n$, are coefficients in the following expansion of $\boldsymbol{x}_k$: $\boldsymbol{x}^k = [y_1 + e_1^k\lambda_1 \quad y_2 + e_2^k\lambda_2 \quad y_n + e_n^k\lambda_n]^{\mathrm{T}}$, $k = 1, 2, \ldots, N$.

The output of our fuzzy system is determined using centroid defuzzification

$$F(\boldsymbol{x}) = \frac{\sum_{j=1}^{N} D_k(\boldsymbol{x})\boldsymbol{R}^k}{\sum_{j=1}^{N} D_k(\boldsymbol{x})} \tag{8}$$

is a realisation of an interpolated coarse model $\bar{\boldsymbol{R}}_{\mathrm{c}}$ (1) and can be written as $\bar{\boldsymbol{R}}_{\mathrm{c}}(\boldsymbol{x}) = F(\boldsymbol{x}, X_{\mathrm{B}}(s(\boldsymbol{x})), R_{\mathrm{B}}(s(\boldsymbol{x})))$ since F is a function of both X_{B} and R_{B}.

For practical aspects of the interpolated coarse models technique see [26]. We note that to reduce the number of evaluations of $\boldsymbol{R}_{\mathrm{c}}$, the interpolated model is implemented as a database of interpolating functions (8), which is updated if the coarse model needs to be evaluated. More specifically, if the evaluation point $\boldsymbol{x}$ belongs to a hypercube for which the interpolating function is already set, $\bar{\boldsymbol{R}}_{\mathrm{c}}$ is obtained as the value of the interpolating function F corresponding to this hypercube. Otherwise, F must be first created, then evaluated, then stored in the database.

Because of the exponential growth of the number of base points for each hypercube with the number of variables n, the interpolation method should not be used for $n > 4$ unless the coarse model is not highly non-linear.

As an illustration, we consider the microstrip notch filter with mitered bends [36] shown in Fig. 4. The design parameters are $\boldsymbol{x} = [L_{\mathrm{c}}\ \ L_{\mathrm{o}}\ \ S_{\mathrm{g}}]^{\mathrm{T}}$ mil. Other parameters are $W = 30$ mil, $H = 10$ mil and $\varepsilon_{\mathrm{r}} = 2.2$ (loss tangent 0.0009). Fine model $\boldsymbol{R}_{\mathrm{f}}$ is simulated in Sonnet *em* [37] with a fine grid of 0.5 mil × 0.5 mil, simulation time 1 h and 34 min (12 points per frequency sweep). The design specifications are $|S_{21}| \geq 0.95$ for $12.7\ \mathrm{GHz} \leq \omega \leq 13.0\ \mathrm{GHz}$, $|S_{21}| \leq 0.05$ for $13.19\ \mathrm{GHz} \leq \omega \leq 13.21\ \mathrm{GHz}$ and $|S_{21}| \geq 0.95$ for $13.4\ \mathrm{GHz} \leq \omega \leq 13.7\ \mathrm{GHz}$.

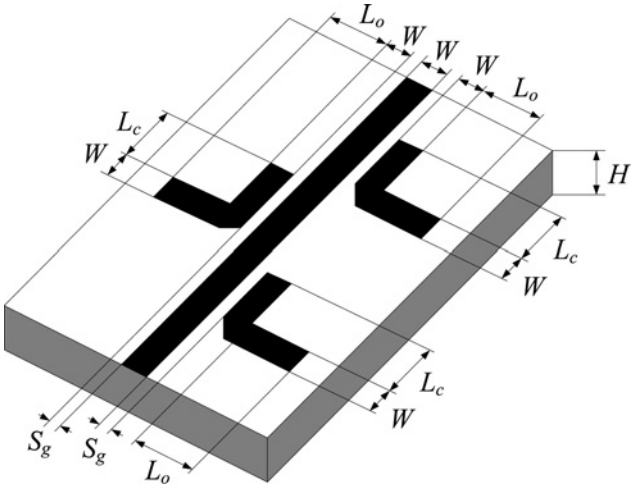

Figure 4 *Microstrip notch filter with mitered bends [36]*

The original coarse model $\boldsymbol{R}_{\mathrm{c}}$ is simulated in Sonnet *em* with a grid of 5 mil × 1 mil, simulation time 65 s. Only being available on a coarse grid, $\boldsymbol{R}_{\mathrm{c}}$ cannot be directly used for optimisation. Instead, we use $\bar{\boldsymbol{R}}_{\mathrm{c}}$, an interpolated model (8) based on $\boldsymbol{R}_{\mathrm{c}}$ with grid size $\boldsymbol{\lambda} = [5\ \ 1\ \ 1]^{\mathrm{T}}$ mil. The optimal solution of this model is $\boldsymbol{x}_1^{(0)} = [145\ \ 158\ \ 8]^{\mathrm{T}}$ mil. See Fig. 5 for the fine and coarse model responses.

We also use $\boldsymbol{R}_{\mathrm{c1}}$, the circuit model implemented in Agilent ADS [38] shown in Fig. 6, evaluation time about 1.5 s. With its substrate permittivity tuned to $\varepsilon_{\mathrm{r}} = 1.46$ this model's centre frequency shifts to 13.2 GHz at $\boldsymbol{x}_1^{(0)}$. Without tuning, the centre frequency of $\boldsymbol{R}_{\mathrm{c1}}$ is about 11.12 GHz, causing severe model misalignment and making $\boldsymbol{R}_{\mathrm{c1}}$ unsuitable for space mapping optimisation. See Fig. 7 for the responses of $\boldsymbol{R}_{\mathrm{c1}}$ at $\boldsymbol{x}_1^{(0)}$ before and after the tuning of ε_{r}.

We employed surrogate model $\boldsymbol{R}_{\mathrm{s}}(\boldsymbol{x}) = \boldsymbol{R}_{\mathrm{c}}(\boldsymbol{x} + \boldsymbol{c}) + \boldsymbol{d}$, where vector $\boldsymbol{c}$ is found using parameter extraction (4), after which $\boldsymbol{d}$ is the residual vector evaluated by $\boldsymbol{d} = \boldsymbol{R}_{\mathrm{f}}(\boldsymbol{x}) - \boldsymbol{R}_{\mathrm{c}}(\boldsymbol{x} + \boldsymbol{c})$. We perform space mapping optimisation twice: using $\bar{\boldsymbol{R}}_{\mathrm{c}}$ with

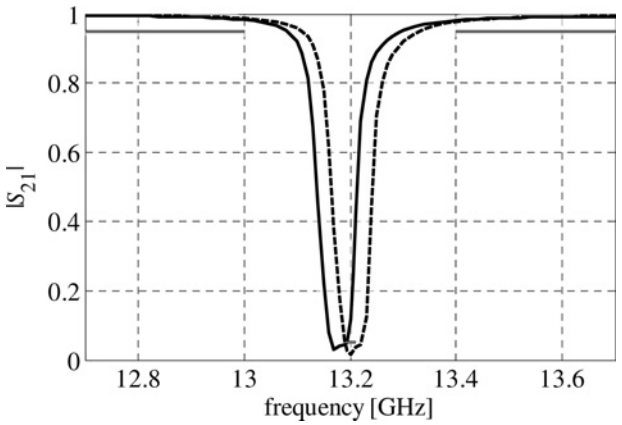

Figure 5 *Microstrip notch filter: the initial fine model response (solid line) and the coarse model $\bar{R}_c$ response (dashed line) at $\boldsymbol{x}_1^{(0)}$ [26]*

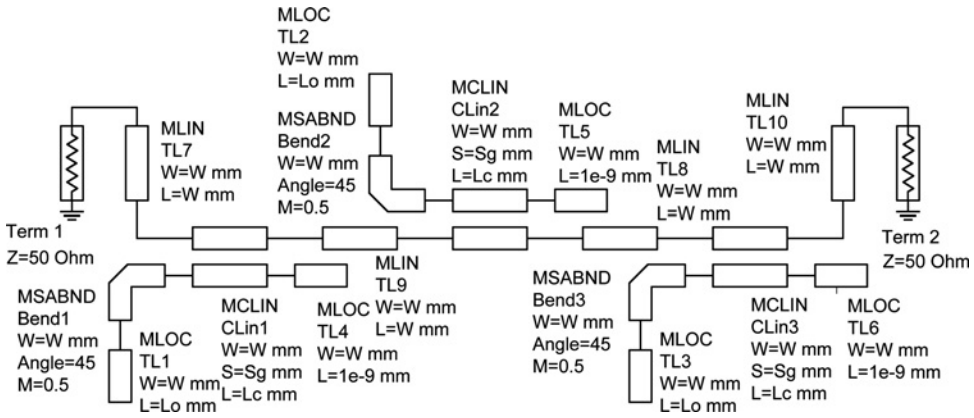

Figure 6 *Coarse model $\boldsymbol{R}_{c1}$ of the notch filter simulated by Agilent ADS [26]*

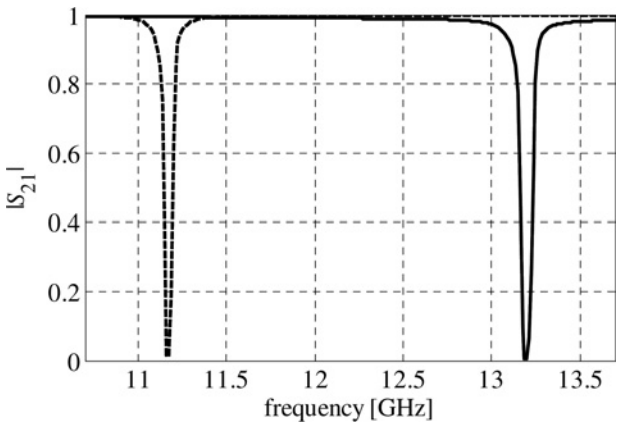

Figure 7 *Microstrip notch filter: response of the coarse model $\boldsymbol{R}_{c1}$ at $\boldsymbol{x}_1^{(0)}$ without tuning of ε_r (dashed line) and with ε_r tuned to 1.46 (solid line) [26]*

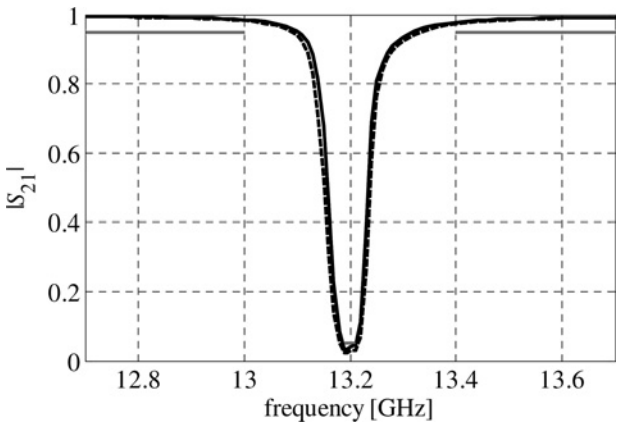

Figure 8 *Microstrip notch filter: the final fine model response at the solution obtained with space mapping using the $\bar{R}_c$ model (solid line) and the $\boldsymbol{R}_{c1}$ model (dashed line) [26]*

starting point $\boldsymbol{x}_1^{(0)}$, then $\boldsymbol{R}_{c1}$ with starting point $\boldsymbol{x}_2^{(0)} = [145\ 158\ 9]^T$, the optimum of the tuned $\boldsymbol{R}_{c1}$.

Table 1 shows the results. The final solutions (see Fig. 8) satisfy the specifications, namely, $[145\ 157.5\ 8]^T$ mil for $\bar{\boldsymbol{R}}_c$ and $[144.5\ 158\ 7]^T$ mil for $\boldsymbol{R}_{c1}$. The cost of space mapping optimisation, however, is substantially smaller for the more accurate $\bar{\boldsymbol{R}}_c$ than for $\boldsymbol{R}_{c1}$. The evaluation time for the original coarse model $\boldsymbol{R}_c$ is 65 s, but because our interpolated model only required 26 evaluations of $\boldsymbol{R}_c$, the total time for parameter extraction and surrogate optimisation is 28 min.

3.2 Multi-coarse-model space mapping

The interpolated coarse model technique can be effectively used only when the number n of design variables is small [26]. We can overcome this drawback through a multi-coarse-model space mapping algorithm [27], which assumes two coarse models: $\boldsymbol{R}_{c1}$ and $\boldsymbol{R}_{c2}$, the first very cheap but not necessarily accurate, the second expensive but significantly more accurate. $\boldsymbol{R}_{c1}$ could be a circuit equivalent, $\boldsymbol{R}_{c2}$ could be implemented with the same

Table 1 Space mapping optimisation results for the microstrip notch filter [26]

Coarse model	Final specification error	Number of fine model evaluations[a]	Total optimisation time	Total fine model evaluation time	Total parameter extraction and surrogate optimisation time
$\bar{\boldsymbol{R}}_c$	−0.006	2	3 h 36 min	3 h 8 min (87%)	28 min (13%)
$\boldsymbol{R}_{c1}$	−0.02	6	9 h 40 min	9 h 24 min (97%)	16 min (3%)

[a]Includes fine model evaluation at the starting point.

IET Microw. Antennas Propag., 2010, Vol. 4, Iss. 4, pp. 453–465

doi: 10.1049/iet-map.2009.0198

simulator as the fine model but using a coarser mesh. We require that a few evaluations of $\boldsymbol{R}_{c2}$ take less time than a single evaluation of $\boldsymbol{R}_f$. According to [27], $\boldsymbol{R}_{c1}$ is enhanced using $\boldsymbol{R}_{c2}$ with a standard space mapping modelling technique [39]. Our enhanced model becomes

$$\boldsymbol{R}_c(\boldsymbol{x}) = \boldsymbol{A} \cdot \boldsymbol{R}_{c1}(\boldsymbol{B} \cdot \boldsymbol{x} + \boldsymbol{c}) \tag{9}$$

with parameters $\boldsymbol{A}$, $\boldsymbol{B}$ and $\boldsymbol{c}$ determined as

$$(\boldsymbol{A}, \boldsymbol{B}, \boldsymbol{c}) = \arg \min_{(\alpha,\beta,\gamma)} \sum_{k=1}^{N} \|\boldsymbol{R}_{c2}(\boldsymbol{x}^k) - \boldsymbol{R}_{c1}(\boldsymbol{x}^k, \boldsymbol{\alpha}, \boldsymbol{\beta}, \boldsymbol{\gamma})\| \tag{10}$$

while $\boldsymbol{x}^k$, $k = 1, 2, \ldots, N$, are base points, for example, the star-distribution [39] with centre at the $\boldsymbol{R}_{c1}$ optimum. Typically, N is between $n+1$ to $2n+1$. If necessary, model (9) can be enhanced by other mappings, for example, a frequency scaling [39].

Our $\boldsymbol{R}_c$, defined by (9) and (10), is as computationally cheap as $\boldsymbol{R}_{c1}$, yet almost as accurate as $\boldsymbol{R}_{c2}$ in the region determined by the base points $\boldsymbol{x}^k$. Both coarse models are taken as physics-based, so we expect a good global match between $\boldsymbol{R}_{c1}$ and $\boldsymbol{R}_{c2}$. The enhanced coarse model is then used in a regular space mapping algorithm.

The algorithm consists of two parts: (i) creating the enhanced $\boldsymbol{R}_c$ and (ii) regular space mapping optimisation (cf. Section 2). It can be described as follows [27]:

Step 1: Optimise $\boldsymbol{R}_{c1}$ to find $\boldsymbol{x}_{c1}^* = \arg\min\{\boldsymbol{x}: U(\boldsymbol{R}_{c1}(\boldsymbol{x}))\}$;

Step 2: Choose a base set $\boldsymbol{x}^k$, $k = 1, \ldots, N$;

Step 3: Evaluate $\boldsymbol{R}_{c2}$ at base points $\boldsymbol{x}^k$, $k = 1, \ldots, N$;

Step 4: Obtain $\boldsymbol{R}_c$ through parameter extraction (10);

Step 5: Find $\boldsymbol{x}^{(0)} = \arg\min\{\boldsymbol{x}: U(\boldsymbol{R}_c(\boldsymbol{x}))\}$;

Step 6: Set $i = 0$;

Step 7: Evaluate the fine model to find $\boldsymbol{R}_f(\boldsymbol{x}^{(i)})$;

Step 8: Obtain the surrogate model $\boldsymbol{R}_s^{(i)}$ using (3) and (4);

Step 9: Given $\boldsymbol{x}^{(i)}$ and $\boldsymbol{R}_s^{(i)}$, obtain $\boldsymbol{x}^{(i+1)}$ using (2);

Step 10: If the termination condition is not satisfied set $i = i + 1$ and go to Step 7; else END;

The size of the region for enhancing the coarse model $\boldsymbol{R}_{c1}$ should be selected as small as possible, however, large enough to make the enhanced model able to satisfy the design specifications within the region. A good indication for the region size would be $\|\bar{\boldsymbol{c}}\|$ where $\bar{\boldsymbol{c}} = \arg\min_c \|\boldsymbol{R}_{c2}(\boldsymbol{x}_{c1}^*) - \boldsymbol{R}_{c1}(\boldsymbol{x}_{c1}^* + \boldsymbol{c})\|$ (here, $\boldsymbol{x}_{c1}^*$ is the optimal solution of $\boldsymbol{R}_{c1}$). For many problems, 10%–20% deviation around $\boldsymbol{x}_{c1}^*$ is sufficient.

For illustration consider the third-order Chebyshev bandpass filter [40] of Fig. 9. Here, the design optimisation parameters are $\boldsymbol{x} = [L_1 \;\; L_2 \;\; S_1 \;\; S_2]^T$ mm. Other parameters are $W_1 = W_2 = 0.4$ mm. The fine model $\boldsymbol{R}_f$ is simulated in Sonnet *em* [37] with a fine grid of 0.2 mm × 0.02 mm, simulation time about 25 min. The design specifications are $|S_{21}| \geq -3$ dB for $1.8 \text{ GHz} \leq \omega \leq 2.2 \text{ GHz}$, and $|S_{21}| \leq -20$ dB for $1.0 \text{ GHz} \leq \omega \leq 1.6 \text{ GHz}$ and $2.4 \text{ GHz} \leq \omega \leq 3.0 \text{ GHz}$. $\boldsymbol{R}_{c1}$ is implemented as a circuit model in Agilent ADS [38] (Fig. 10), evaluation time about 1.5 s. $\boldsymbol{R}_{c2}$ is simulated in Sonnet *em* with a coarse grid of 2 mm × 0.1 mm, simulation time about 1 min.

We performed standard space mapping with $\boldsymbol{R}_{c1}$ as well as with the multi-coarse-model approach. $\boldsymbol{R}_c$ was enhanced as described in Section 2 using input and frequency space mapping and the star-distribution base set requiring nine evaluations of $\boldsymbol{R}_{c2}$. The evaluation time for $\boldsymbol{R}_c$ is similar to that for $\boldsymbol{R}_{c1}$, about 1.5 s. Our optimisation process used the input surrogate $\boldsymbol{R}_s(\boldsymbol{x}) = \boldsymbol{R}_c(\boldsymbol{x} + \boldsymbol{c})$ enhanced by frequency space mapping [39].

Table 2 shows that the multi-coarse-model approach produces a better solution than standard space mapping for a smaller number of fine model evaluations. Fig. 11 shows various responses at the optimal solution of $\boldsymbol{R}_{c1}$, $\boldsymbol{x}_{c1}^* = [14.6 \;\; 15.2 \;\; 0.56 \;\; 0.54]^T$ mm. Note that $\boldsymbol{R}_c$ provides a better match to the fine model than $\boldsymbol{R}_{c1}$ and hence better performance of the algorithm. Fig. 12 shows $\boldsymbol{R}_f$ at the final solution $\boldsymbol{x}^* = [14.8 \;\; 14.8 \;\; 0.40 \;\; 0.84]^T$ mm.

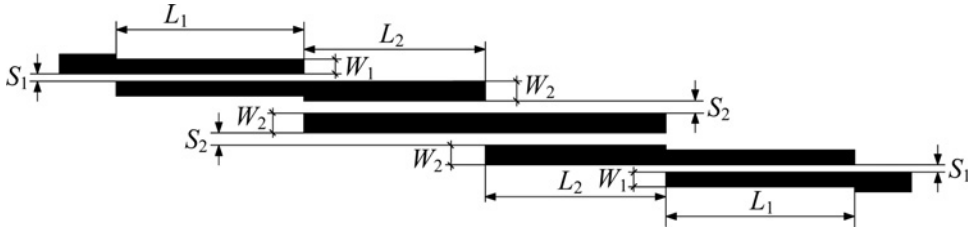

Figure 9 *Third-order Chebyshev bandpass filter [40]*

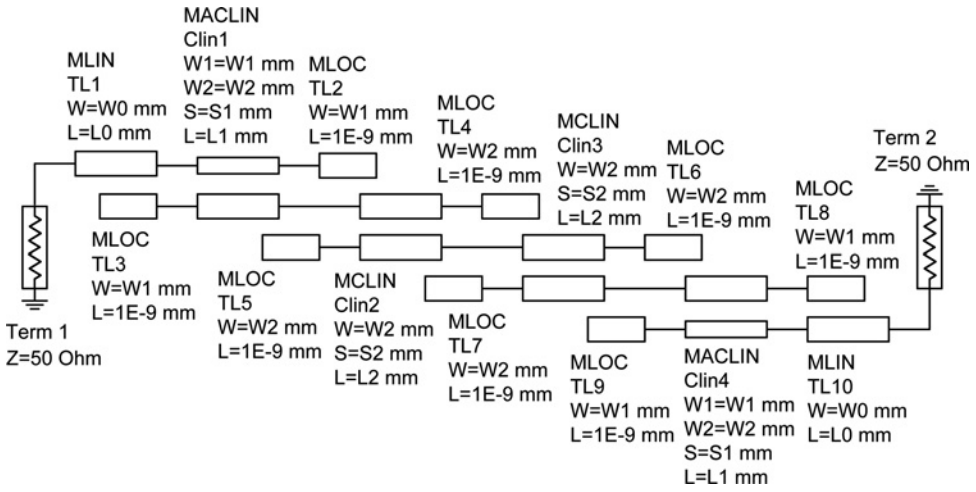

Figure 10 *Coarse model R_{c1} of the third-order Chebyshev filter (Agilent ADS) [27]*

Table 2 Results for third-order Chebyshev microstrip filter [27]

Algorithm	Final specification error, dB	Number of fine model evaluations[a]
standard SM algorithm with coarse model R_{c1}	−0.4	5
multi-coarse-model SM algorithm with models R_{c1} and R_{c2}	−1.5	3

[a]Excludes fine model evaluation at the starting point.

3.3 Exploiting built-in optimisation capabilities of the coarse model simulator

Agilent ADS [38] is widely used by the microwave community as it allows convenient, straightforward creation of coarse models for relevant devices.

Although the actual Advanced Design System (ADS) simulation time might be very short (for example, a few milliseconds), the whole process of evaluating the coarse model by an optimisation routine repeatedly calling the simulator whereas solving problems (2) or (4) is much longer (for example, a few seconds) because of the additional cost related to preparing the input data, loading the simulator into memory and so on.

In a standard implementation of the space mapping optimisation algorithm, both the parameter extraction and surrogate model optimisation sub-problems are solved using optimisation routines that call the coarse model simulator whenever the coarse model has to be evaluated. Here, we use Matlab's Optimisation Toolbox [41], in particular fmincon or lsqnonlin for parameter extraction, and fminimax

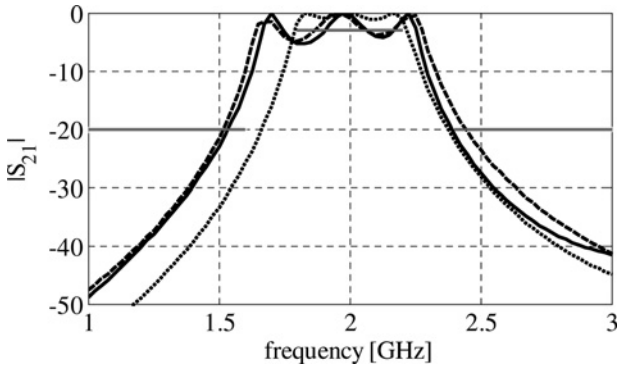

Figure 11 *Third-order Chebyshev filter: the fine model R_f response (solid line), coarse model R_{c1} response (dotted line) and enhanced coarse model R_c response (dashed line) at x_{c1}^* [27]*

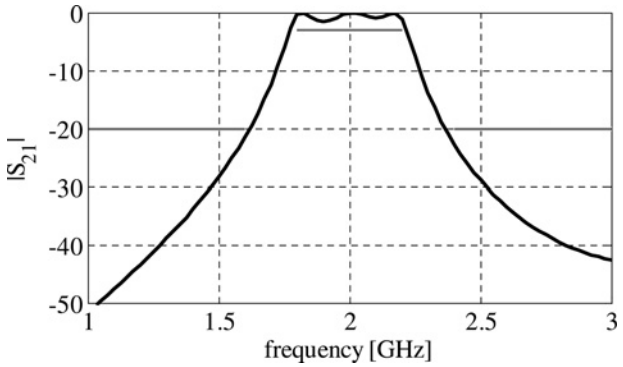

Figure 12 *Third-order Chebyshev filter: the final fine model response at the solution obtained with the multi-coarse-model algorithm [27]*

for surrogate optimisation. When we invoke ADS, CPU clock cycles are consumed on allocating memory, loading the simulator, verifying the license, loading the input file, parsing the input file, simulating the circuit, exporting the response and so on. Whereas circuit simulation may be fast

doi: 10.1049/iet-map.2009.0198

for a single design, repeatedly invoking ADS generates a significant overhead.

Fig. 13 shows the interaction between the optimisation routine and ADS within the standard implementation of the space mapping algorithm. For k evaluations of the coarse model for either parameter extraction or surrogate optimisation, the total optimisation time would be $k(t_o + t_s)$, where t_o is the overhead time, and t_s is the simulation time for a single design. Here, t_s may be a few milliseconds, whereas t_o might be as large as a few seconds, so that we have $t_s \ll t_o$.

Since typical surrogate optimisation requires dozens or hundreds, whereas parameter extraction (especially multi-point) even thousands of coarse model evaluations, the overhead may be substantial. The relative overhead may be even more significant if techniques such as parallel or distributed fine model evaluations are used that reduce the evaluation time of the fine model. In such cases, the total coarse model evaluation time may even dominate the execution time of the space mapping algorithm.

In [28], both parameter extraction and surrogate model optimisation are carried out inside ADS using its internal optimisation capabilities. Because the optimisation loop is moved into ADS, the space mapping algorithm prepares only the modified ADS netlist and initiates one call to ADS for the entire optimisation process, thus saving significant time.

The netlist is now enhanced by DAC components that import multiple designs and corresponding fine model responses, by VAR components incorporating space mapping equations and matrices, by optimisation GOAL components specifying matching goals between fine and surrogate models, and by optimisation engine OPTIM that searches for the optimal solution for parameter extraction.

In accordance with the type of optimisation sub-problem that requires to be solved, netlist modifications for the parameter extraction step and the surrogate model optimisation step are different. Fig. 14 outlines the appropriate inside-ADS optimisation approach. The coarse model netlist is modified once for a single ADS call. For any k evaluations of the coarse model, the total optimisation time would be $t_o' + k \cdot t_s'$, where t_o' is the overhead time, and t_s' is the circuit simulation time for a modified design. The t_o' and t_s' are different from t_o and t_s, respectively, but are of the same orders of magnitude, namely, milliseconds and seconds, respectively, hence the efficiency of inside-ADS optimisation.

Consider the bandpass microstrip filter with open stub inverter [42] of Fig. 15. The design parameters are $\boldsymbol{x} = [L_1\ L_2\ L_3\ S_1\ S_2\ W_1]^T$. The fine model is simulated in FEKO [43]. The design specifications are $|S_{21}| \leq -20$ dB for 1.5 GHz $\leq \omega \leq$ 1.8 GHz, $|S_{21}| \geq -3$ dB for 1.95 GHz $\leq \omega \leq$ 2.05 GHz and $|S_{21}| \leq -20$ dB for 2.2 GHz $\leq \omega \leq$ 2.5 GHz, where S_{21} is the complex transmission coefficient between the input and output ports. $|S_{21}|$ is evaluated at 41 frequency points uniformly distributed in the interval 1.5–2.5 GHz. The coarse model implemented in Agilent ADS [38] is shown in Fig. 16, with corresponding optimal solution $\boldsymbol{x}^{(0)} = [25.00\ \ 5.00\ \ 1.221\ \ 0.652\ \ 0.187\ \ 0.100]^T$ mm and specification error + 15.7 dB.

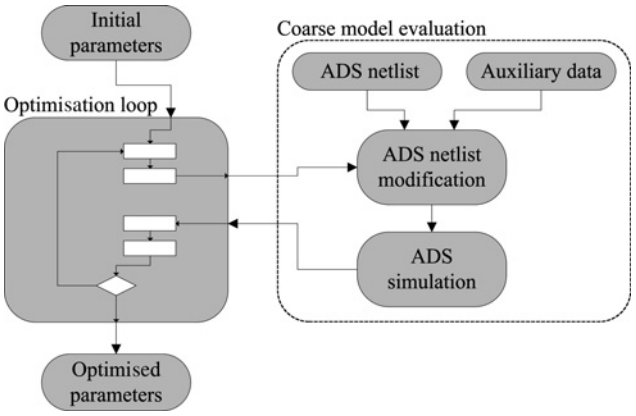

Figure 13 *Standard implementation of the space mapping algorithm with ADS*

Initial/optimised parameters are space mapping parameters during parameter extraction and design variables during surrogate optimisation. Auxiliary data include design specifications, space mapping formulas and setup data. The optimisation routine considers ADS an external function evaluator (repeatedly called) with the coarse model netlist modified to correspond to the current design

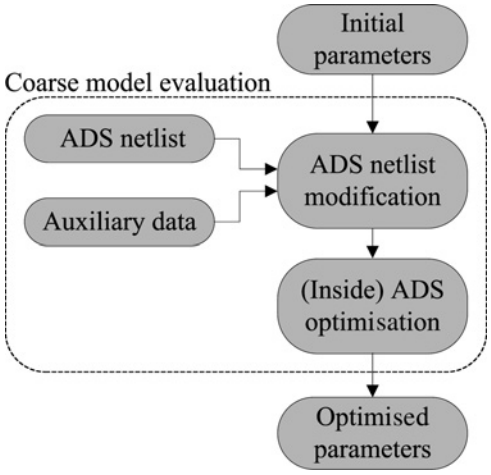

Figure 14 *Inside-ADS parameter extraction and surrogate optimisation*

The initial/optimised parameters are either space mapping parameters or design variables according to the sub-problem considered. Auxiliary data include design specifications, space mapping formulas and setup data. For each sub-problem, ADS is called just once with an appropriately modified coarse model netlist

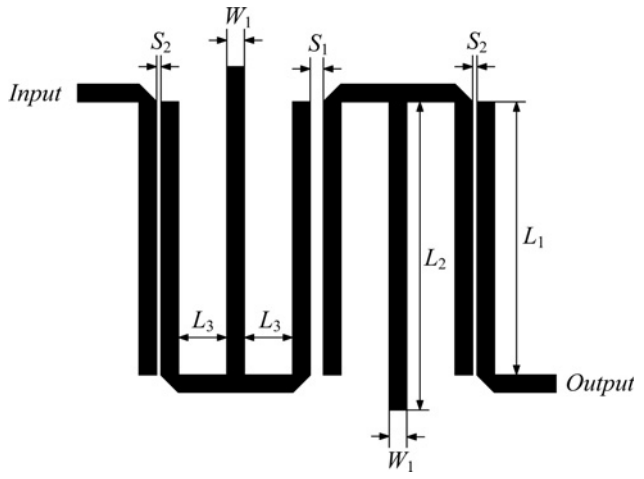

Figure 15 *Geometry of the bandpass filter with open stub inverter [42]*

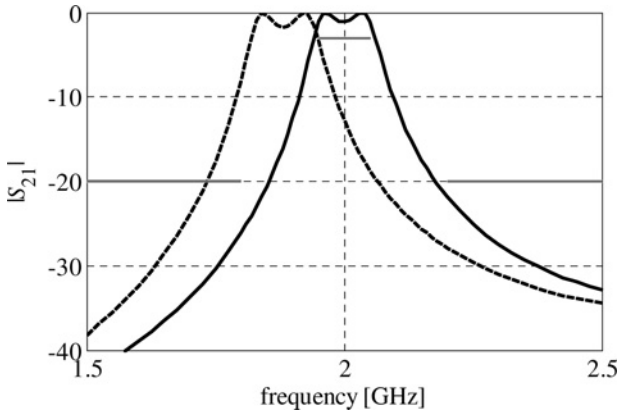

Figure 17 *Initial (dashed line) and optimised (solid line) $|S_{21}|$ against frequency for the bandpass filter with open stub inverter [44]*

Our surrogate model $\bar{\boldsymbol{R}}_s(\boldsymbol{x}, \boldsymbol{p}) = \bar{\boldsymbol{R}}_s(\boldsymbol{x}, \boldsymbol{F}, \boldsymbol{c}, \boldsymbol{d}) = \boldsymbol{R}_{c.f}(\boldsymbol{x} + \boldsymbol{c}) + \boldsymbol{d}$ corresponds to input, frequency [39] and output space mappings, where $\boldsymbol{R}_{c.f}$ is the coarse model that is evaluated at frequencies different from the original frequency sweep obtained from the mapping $\omega \rightarrow f_1 + f_2 \cdot \omega$, with $\boldsymbol{F} = [f_1 \; f_2]^T$, whereas output parameter $\boldsymbol{d}$ is calculated as $\boldsymbol{d} = \boldsymbol{R}_f(\boldsymbol{x}) - \boldsymbol{R}_{c.f}(\boldsymbol{x} + \boldsymbol{c})$ after parameters $\boldsymbol{c}$ and $\boldsymbol{F}$ are extracted. Fig. 17 shows the fine model response at $\boldsymbol{x}^{(0)}$ and the optimised fine model response after four space mapping iterations at $\boldsymbol{x}^{(4)} = [23.64 \;\; 5.00 \;\; 1.00 \;\; 0.742 \;\; 0.189 \;\; 0.100]^T$ mm. The specification error is −1.9 dB.

Table 3 compares the three implementations of the space mapping algorithm. For the standard implementation, the cost is mostly due to fine model evaluation (about 36 min per evaluation on a Pentium D 3.4 GHz processor). The relative contribution of coarse model evaluation from solving the parameter extraction and surrogate optimisation sub-problems is insignificant.

The same space mapping algorithm was also run with the distributed fine model evaluation [44] implemented in the SMF system [29]. This allowed us to reduce each fine model evaluation to about 3 min. The fine model was evaluated on a cluster of 14 processors: 1 Pentium D 3.4 GHz and 13 nodes of the computing cluster containing Dual Core AMD 2 GHz processors and Intel Xeon 3.06 GHz processors. The total fine model evaluation is reduced from 181 to 16 min and the parameter extraction and surrogate optimisation sub-problems now cost almost 80% of the total cost.

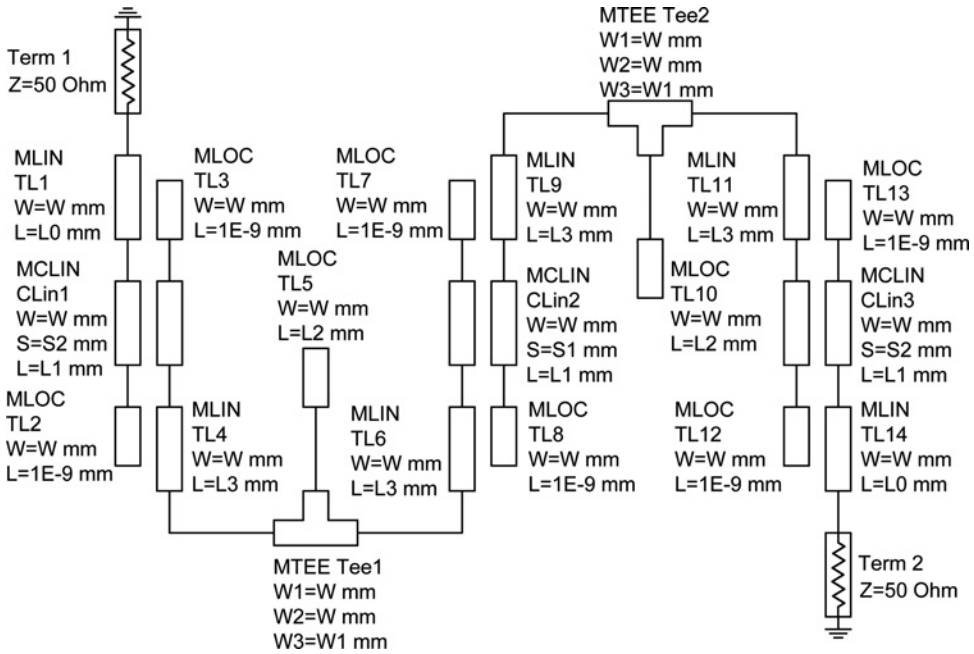

Figure 16 *Coarse model of the bandpass filter with open stub inverter simulated by Agilent ADS [44]*

doi: 10.1049/iet-map.2009.0198

Table 3 Bandpass filter with open stub inverter: optimisation time for the three implementations of the space mapping algorithm [44]

Space mapping algorithm	Total optimisation time, min	Fine model evaluation time		Parameter extraction and surrogate model optimisation time	
		Absolute, min	Relative, %	Absolute, min	Relative, %
standard implementation	241	181	75	60	25
distributed fine model evaluation [44]	76	16	21	60	79
distributed fine model evaluation [44] and inside-ADS optimisation	19	16	84	3	16

Our inside-ADS process allows us to reduce the parameter extraction and surrogate optimisation overhead from 60 min to about 3 min and the space mapping optimisation time to 19 min. In this case, the total relative cost of evaluating the coarse model is only 16%, which is exactly what one would like to see in a well-performing space mapping algorithm.

The difference in solving the relevant sub-problems between the standard implementation and the inside-ADS optimisation is not as large as could be expected by comparing t_s with t_o (milliseconds against a few seconds). This is because the number of objective function evaluations necessary to complete the process is generally larger for ADS than for Matlab (different optimisation routines).

4 Conclusion

We have discussed the importance of the coarse model in the performance of the space mapping optimisation process. Various techniques for enhancing the efficiency of space mapping algorithms by increasing the speed and accuracy of the underlying coarse model have been reviewed and illustrated using several microwave design problems. It has been shown that the combination of a more accurate but also computationally more expensive coarse model with a less accurate but computationally cheap circuit-equivalent coarse model and/or suitable interpolation/approximation techniques allows us to obtain a reasonable trade-off between accuracy and the computational cost of the coarse model, and thus improve the overall performance of the space mapping optimisation algorithm. On the other hand, we demonstrated substantial performance improvement by exploiting the built-in optimisation capabilities of the model evaluator (here, Agilent ADS) that can be used instead of the external optimisation routines.

5 Acknowledgment

The authors thank Sonnet Software, Inc., Syracuse, NY, for *em*™ and Agilent Technologies, Santa Rosa, CA, for making ADS available. This work was supported in part by the Reykjavik University Development Fund and the Natural Sciences and Engineering Research Council of Canada under Grants RGPIN7239-06 and STPGP336760-06.

6 References

[1] QUEIPO N.V., HAFTKA R.T., SHYY W., GOEL T., VAIDYNATHAN R., TUCKER P.K.: 'Surrogate-based analysis and optimization', *Prog. Aerosp. Sci.*, 2005, **41**, (1), pp. 1–28

[2] ALEXANDROV N.M., LEWIS R.M.: 'An overview of first-order model management for engineering optimization', *Optim. Eng.*, 2001, **2**, (4), pp. 413–430

[3] BOOKER A.J., DENNIS JR. J.E., FRANK P.D., SERAFINI D.B., TORCZON V., TROSSET M.W.: 'A rigorous framework for optimization of expensive functions by surrogates', *Struct. Optim.*, 1999, **17**, (1), pp. 1–13

[4] MYERS R.H., MONTGOMERY D.C.: 'Response surface methodology' (Wiley, 2002)

[5] BANDLER J.W., BIERNACKI R.M., CHEN S.H., GROBELNY P.A., HEMMERS R.H.: 'Space mapping technique for electromagnetic optimization', *IEEE Trans. Microw. Theory Tech.*, 1994, **4**, (12), pp. 536–544

[6] BANDLER J.W., CHENG Q.S., DAKROURY S.A., MOHAMED A.S., BAKR M.H., MADSEN K., SØNDERGAARD J.: 'Space mapping: the state of the art', *IEEE Trans. Microw. Theory Tech.*, 2004, **52**, (1), pp. 337–361

[7] KOZIEL S., BANDLER J.W., MADSEN K.: 'A space mapping framework for engineering optimization: theory and implementation', *IEEE Trans. Microw. Theory Tech.*, 2006, **54**, (10), pp. 3721–3730

[8] ECHEVERRIA D., HEMKER P.W.: 'Space mapping and defect correction', *CMAM Int. Math. J. Comput. Methods Appl. Math.*, 2005, **5**, (2), pp. 107–136

[9] ISMAIL M.A., SMITH D., PANARIELLO A., WANG Y., YU M.: 'EM-based design of large-scale dielectric-resonator filters and

multiplexers by space mapping', *IEEE Trans. Microw. Theory Tech.*, 2004, **52**, (1), pp. 386–392

[10] AMARI S., LEDREW C., MENZEL W.: 'Space-mapping optimization of planar coupled-resonator microwave filters', *IEEE Trans. Microw. Theory Tech.*, 2006, **54**, (5), pp. 2153–2159

[11] CREVECOEUR G., DUPRE L., VAN DE WALLE R.: 'Space mapping optimization of the magnetic circuit of electrical machines including local material degradation', *IEEE Trans. Magn.*, 2007, **43**, (6), pp. 2609–2611

[12] LEARY S.J., BHASKAR A., KEANE A.J.: 'A constraint mapping approach to the structural optimization of an expensive model using surrogates', *Optim. Eng.*, 2001, **2**, (4), pp. 385–398

[13] REDHE M., NILSSON L.: 'Using space mapping and surrogate models to optimize vehicle crashworthiness design'. Ninth AIAA/ISSMO Multidisciplinary Analysis and Optimization Symp., Atlanta, GA, September 2002, Paper AIAA-2002-5536

[14] CHOI H.-S., KIM D.H., PARK I.H., HAHN S.Y.: 'A new design technique of magnetic systems using space mapping algorithm', *IEEE Trans. Magn.*, 2001, **37**, (5), pp. 3627–3630

[15] POWELL M.J.D.: 'Radial basis functions for multivariate interpolation: a review', in MASON J.C., COX M.G. (EDS.): 'Algorithms for approximation' (Clarendon Press, Oxford, 1987)

[16] SIMPSON T.W., MAUREY T.M., KORTE J.J., MISTREE F.: 'Kriging models for global approximation in simulation-based multidisciplinary design optimization', *AIAA J.*, 2001, **39**, (12), pp. 2233–2241

[17] SIMPSON T.W., PEPLINSKI J., KOCH P.N., ALLEN J.K.: 'Metamodels for computer-based engineering design: survey and recommendations', *Eng. Comput.*, 2001, **17**, (2), pp. 129–150

[18] LEARY S.J., BHASKAR A., KEANE A.J.: 'A knowledge-based approach to response surface modeling in multifidelity optimization', *Global Optim.*, 2003, **26**, (3), pp. 297–319

[19] MORRO J.V., ESTEBAN H., BORIA V.E., BACHILLER C., COVES A.: 'New multimodel ASM technique for the efficient design of complex microwave circuits'. IEEE MTT-S Int. Microwave Symp. Dig., Long Beach, CA, June 2005, pp. 1613–1616

[20] MENG J., KOZIEL S., BANDLER J.W., BAKR M.H., CHENG Q.S.: 'Tuning space mapping: a novel technique for engineering design optimization'. IEEE MTT-S Int. Microwave Symp. Dig., Atlanta, GA, June 2008, pp. 991–994

[21] KOZIEL S., BANDLER J.W.: 'Controlling convergence of space-mapping algorithms for engineering optimization'. Int. Symp. Signals, Systems and Electronics, URSI ISSSE 2007, Montreal, Canada, 2007, pp. 21–23

[22] KOZIEL S., BANDLER J.W., CHENG Q.S.: 'Adaptive space mapping with convergence enhancement for optimization of microwave structures and devices'. IEEE MTT-S Int. Microwave Symp. Dig., Atlanta, GA, June 2008, pp. 987–990

[23] KOZIEL S., BANDLER J.W., MADSEN K.: 'Quality assessment of coarse models and surrogates for space mapping optimization', *Optim. Eng.*, 2008, **9**, (4), pp. 375–391

[24] KOZIEL S., BANDLER J.W.: 'Space-mapping optimization with adaptive surrogate model', *IEEE Trans. Microw. Theory Tech.*, 2007, **55**, (3), pp. 541–547

[25] KOZIEL S., BANDLER J.W.: 'Coarse and surrogate model assessment for engineering design optimization with space mapping'. IEEE MTT-S Int. Microwave Symp. Dig., Honolulu, HI, June 2007, pp. 107–110

[26] KOZIEL S., BANDLER J.W.: 'Interpolated coarse models for microwave design optimization with space-mapping', *IEEE Trans. Microw. Theory Tech.*, 2007, **55**, (8), pp. 1739–1746

[27] KOZIEL S., BANDLER J.W.: 'Space mapping with multiple coarse models for optimization of microwave components', *IEEE Microw. Wirel. Compon. Lett.*, 2008, **18**, (1), pp. 1–3

[28] KOZIEL S., CHENG Q.S., BANDLER J.W.: 'Improving efficiency of space mapping optimization of microwave structures and devices'. IEEE MTT-S Int. Microwave Symp. Dig., Honolulu, HI, June 2007, pp. 1995–1998

[29] KOZIEL S., BANDLER J.W.: 'SMF: a user-friendly software engine for space-mapping-based engineering design optimization'. Int. Symp. Signals, Systems and Electronics, URSI ISSSE 2007, Montreal, Canada, 2007, pp. 157–160

[30] CHENG Q.S., BANDLER J.W., KOZIEL S.: 'Combining coarse and fine models for optimal design', *Microw. Mag.*, 2008, **9**, (1), pp. 79–88

[31] ZHU J., BANDLER J.W., NIKOLOVA N.K., KOZIEL S.: 'Antenna optimization through space mapping', *IEEE Trans. Antennas Propag.*, 2007, **55**, (3), pp. 651–658

[32] MIRAFTAB V., MANSOUR R.R.: 'Computer-aided tuning of microwave filters using fuzzy logic', *IEEE Trans. Microw. Theory Tech.*, 2002, **50**, (12), pp. 2781–2788

[33] MIRAFTAB V., MANSOUR R.R.: 'A robust fuzzy-logic technique for computer-aided diagnosis of microwave filters', *IEEE Trans. Microw. Theory Tech.*, 2004, **52**, (1), pp. 450–456

[34] MIRAFTAB V., MANSOUR R.R.: 'EM-based microwave circuit design using fuzzy logic techniques', *IEE Proc. Microw. Antennas Propag.*, 2006, **153**, (6), pp. 495–501

doi: 10.1049/iet-map.2009.0198

[35] WANG L.-X., MENDEL J.M.: 'Generating fuzzy rules by learning from examples', *IEEE Trans. Systems Man. Cybern.*, 1992, **22**, (6), pp. 1414–1427

[36] RAYAS-SÁNCHEZ J.E., GUTIÉRREZ-AYALA V.: 'EM-based Monte Carlo analysis and yield prediction of microwave circuits using linear-input neural-output space mapping', *IEEE Trans. Microw. Theory Tech.*, 2006, **54**, (12), pp. 4528–4537

[37] ***em***™ Version 11.53, Sonnet Software, Inc., 100 Elwood Davis Road, North Syracuse, NY 13212, USA, 2008

[38] Agilent ADS, Version 2008, Agilent Technologies, 1400 Fountaingrove Parkway, Santa Rosa, CA 95403-1799, 2008

[39] KOZIEL S., BANDLER J.W., MOHAMED A.S., MADSEN K.: 'Enhanced surrogate models for statistical design exploiting space mapping technology'. IEEE MTT-S Int. Microwave Symp. Dig., Long Beach, CA, June 2005, pp. 1609–1612

[40] KUO J.T., CHEN S.P., JIANG M.: 'Parallel-coupled microstrip filters with over-coupled end stages for suppression of spurious responses', *IEEE Microw. Wirel. Compon. Lett.*, 2003, **13**, (10), pp. 440–442

[41] Matlab™, Version 7.6, The MathWorks, Inc., 3 Apple Hill Drive, Natick, MA 01760-2098, 2008

[42] LEE J.R., CHO J.H., YUN S.W.: 'New compact bandpass filter using microstrip $\lambda/4$ resonators with open stub inverter', *IEEE Microw. Guided Wave Lett.*, 2000, **10**, (12), pp. 526–527

[43] FEKO® User's Manual, Suite 5.3, EM Software & Systems-S.A. (Pty) Ltd, 32 Techno Lane, Technopark, Stellenbosch, 7600, South Africa, http://www.feko.info, 2008

[44] KOZIEL S., BANDLER J.W.: 'Distributed fine model evaluation for rapid space mapping optimization of microwave structures', *IET Microw. Antennas Propag.*, 2009, **3**, (5), pp. 798–807